Westphal, A., Lerm, S., Miethling-Graff, R., Seibt, A., Wolfgramm, M., Würdemann, H. (2016): Effects of plant downtime on the microbial community composition in the highly saline brine of a geothermal plant in the North German Basin. - *Applied Microbiology and Biotechnology*, *100*, 7, pp. 3277—3290.

DOI: http://doi.org/10.1007/s00253-015-7181-1

Effects of plant downtime on the microbial community composition in the highly saline brine of a geothermal plant in the North German Basin

Anke Westphal[a], Stephanie Lerm[a], Rona Miethling-Graff[a], Andrea Seibt[b], Markus Wolfgramm[c], Hilke Würdemann[ad]#

[a] GFZ German Research Centre for Geosciences, Section 4.5 Geomicrobiology, 14473 Potsdam, Germany

[b] BWG Geochemische Beratung GmbH, 17041 Neubrandenburg, Germany

[c] Geothermie Neubrandenburg (GTN), 17041 Neubrandenburg, Germany

[d] Environmental Technology, Water- and Recycling Technology, Department of Engineering and Natural Sciences, University of Applied Sciences Merseburg, 06217 Merseburg, Germany

Address correspondence to Hilke Würdemann
wuerdemann@gfz-potsdam.de
Phone: +49 331 288 1516
Fax: ++49 331 2300662

Abstract

The microbial biocenosis in highly saline fluids produced from the cold well of a deep geothermal heat store located in the North German Basin was characterized during regular plant operation and immediately after plant downtime phases. Genetic fingerprinting revealed the dominance of sulfate-reducing bacteria (SRB) and fermentative *Halanaerobiaceae* during regular plant operation, whereas after shut-down phases, sequences of sulfur-oxidizing bacteria (SOB) were also detected. The detection of SOB indicated oxygen ingress into the well during the downtime phase. High 16S rRNA and *dsr*A gene copy numbers at the beginning of the restart process showed an enrichment of *Bacteria*, SRB, and SOB during stagnant conditions consistent with higher concentrations of dissolved organic carbon (DOC), sulfate, and hydrogen sulfide in the produced fluids. The interaction of SRB and SOB during plant downtimes might have enhanced the corrosion processes occurring in the well. It was shown that scale content of fluids was significantly increased after stagnant phases. Moreover, the sulfur isotopic signature of the mineral scales indicated microbial influence on scale formation.

Keywords: geothermal, aquifer, microbial community, SOB, SRB, corrosion

Introduction

Deep terrestrial aquifers contain diverse microbial communities. Analyses of 16S rRNA genes and cultivation-based analyses of anoxic habitats have revealed a wide variety of phylogenetically and physiologically diverse microorganisms, including nitrate reducers, iron reducing bacteria, sulfate reducing bacteria (SRB), fermentative organisms, homoacetogens, methanotrophs, hydrogenotrophic, and aceticlastic methanogens (Stevens and McKinley 1995; Pedersen 1997; Amend and Teske 2005). For deep marine subsurfaces and terrestrial groundwater environments, differences in the community composition and structure can be correlated with physical-chemical conditions, such as temperature, salinity, pH, sulfate concentration, and the availability of organic matter (Griebler and Lueders 2009; Molari et al. 2012). However, factors controlling the spatial and temporal dynamics of microbial community composition are poorly documented for deep terrestrial aquifers. Thus, the quantification of these species and determination of the mutual relationships and interactions might be a challenging task for the present and prospective use as well as planning and monitoring of the subsurface (Bauer et al. 2013).

Microbial communities in aquifers catalyze a broad range of geochemical reactions that can adversely affect the infrastructure and operation of geothermal plants, which access the aquifer through boreholes (or 'wells'). These reactions can lead to corrosion and scaling (Valdez et al. 2009; Javaherdashti 2011). Therefore, the detrimental effect of microbes on geothermal plant components has increasingly attracted attention. Indeed, several studies have been conducted to identify the organisms responsible for phenomena such as scaling, biofouling, and plant infrastructure corrosion (Sand 2003; Valdez et al. 2009; Lerm et al. 2011a; b; Lerm et al. 2013), as these microbial induced processes can lead to plant downtimes and the cost-intensive replacement of plant components (Gallup 2009; Valdez et al. 2009; Miranda-Herrera et al. 2010).

Corrosion leads to the degradation of construction materials and functional loss of technical components, e.g., well casing and submersible pumps. Due to their high chloride concentration, brines themselves are very corrosive fluids and cause pitting corrosion. Many studies have identified different genera of SRB as one of the main factors accelerating corrosion (Hamilton 1985; Lee et al. 1995; Javaherdashti 2011). The effect of SRB activity on the corrosion processes is well known and can significantly increase the steel corrosion rate (Valdez et al. 2009). In addition, organic and inorganic acids produced by bacteria, such as fermentative and sulfur-oxidizing bacteria (SOB), adversely affect metal surfaces and might contribute to the corrosion of metallic construction materials (Javaherdashti 2008). However, questions

concerning the underlying mechanism remain (Enning and Garrelfs 2014).

Scaling in geothermal plants primarily reflects pressure decreases, temperature changes, and/or corrosion, changing the physicochemical conditions in the fluid (Corsi 1986). In addition to reducing the efficiency of pumps, heat exchangers, and turbines, scaling influences the effectiveness of wells, as iron and other metallic cations are enriched through precipitation, leading to the formation of amorphous or crystalline structures that contribute to a continuous decrease in pumping capacity and eventual clogging of the well (Houben and Weihe 2010; Van Beek 1989). Biofouling refers to the accumulation of microorganisms that produce extracellular polymers and form complex biofilms with mineral deposits and adversely affect the hydraulic characteristics of water flow by causing a decrease in the matrix pore spaces in shallow groundwater aquifers (Howsam 1988).

Deep geothermal reservoirs of the North German Basin typically have high temperatures and saline formation waters, creating harsh conditions for the plant equipment. These characteristics can be associated with high corrosion rates consistent with plant downtimes (Fichter et al. 2011).

The fluid samples analyzed in this study were taken from the geothermal heat store in Neubrandenburg, Germany operated at temperatures ranging from 47 °C to 87 °C. Lerm et al. (2013) revealed distinct microbial communities in geothermal fluids produced from the cold and the warm side of the aquifer. In addition, despite short retention times in the heat exchanger a shift in the microbial community composition and higher bacterial gene copy numbers were observed in fluids in consequence of heat extraction. This is regarded as a result of biofilms that established on the heat exchanger plates as well as the downstream piping due to the temperature decrease and were detached with the fluid flow (Lerm et al. 2013).

In the present study, we focused on plant downtimes and monitored variations in microbial communities in the fluids produced from the cold well and the effects of plant downtimes on microbial induced corrosion (MIC). Fluids and filter bags were sampled before and after downtime phases over a period of four years. Shifts in the microbial community structures of the fluids produced after downtime phases were monitored using 16S rDNA-based fingerprinting and quantitative PCR. Consistent with geochemical and mineralogical data, these molecular analyses facilitated the identification of specific microbial metabolic groups that benefited from shutdown phases and provided insight into the processes occurring downhole with respect to corrosion and scaling.

Materials and methods

Site description and plant design

The investigated geothermal plant, located in Neubrandenburg (North German Basin, Germany), is used for seasonal heat storage since 2004. The target sandstone formation is situated at 1,228 - 1,268 m depths and is accessed using a geothermal doublet. The distance between the two wells (GtN 1/86, GtN 4/86) used for both fluid production and injection is approximately 1,300 m.

Fluid from well GtN 4/86 was charged with excess heat from a local gas and steam cogeneration plant during summer (April till November) and subsequently injected via well GtN 1/86 into the aquifer (charge mode). This area is called the "warm well" as the fluid temperature in the aquifer surrounding well GtN 1/86 increased from 54 °C to a final temperature of 87 °C during geothermal plant operation. The second well, GtN 4/86, is called the "cold well" due to the operational caused temperature decrease. During winter time (November till April), fluid produced from the warm well that is used for district heating was subsequently injected into the "cold well" with a temperature of 45 °C to 54 °C (discharge mode).

Both wells and the topside facility were maintained under nitrogen pressure (~10 bar) to reduce precipitation, degassing, and oxygen ingress. Upstream of the heat exchanger, filter systems are installed on the cold as well as on the warm side to retain solid particles emerging in the well and transported with the produced fluid from the aquifer. Furthermore, pumps as well as production and injection pipes are installed on both sides. The average fluid flow rate during regular operation in the plant was 80 $m^3\ h^{-1}$, while the fluid flow rate during plant restart was remarkably lower and varied between 20 $m^3\ h^{-1}$ and 60 $m^3\ h^{-1}$. The borehole volume is 35 m^3. Further information dealing with plant operations and energetics is provided in Kabus and Wolfgramm (2009) and Obst and Wolfgramm (2010). In 2008, 2009, and 2011, plant operation was impaired due to the corrosion damage of a submersible pump in the cold well and the decreased injection rate in the cold well resulting from precipitation and scaling, which led to downtime phases lasting up to three months. Based on the observations in 2008 and 2009, restart processes occurring in 2011 were intensively monitored.

Sample collection

Fluid and filter samples were taken over a period of four years from the two wells and from filter devices at the topside facilities of the heat store. This period included phases of regular plant operation with charge and discharge mode and plant downtime phases lasting up to three months.

Filter samples were collected to analyze the content of solids in the transported fluids and to characterize the scales. Filters were placed in a filter device that contained 2 x 4 filters (Eaton DuraGaf POXL-1-P02E-20l, Lenntech, Delft, Netherlands) with 1-micron ratings. Filters were regularly replaced after a certain filter lifetime (definite volume of fluid passed through). If the injection pressure increased, e.g., due to high particle loading rate after plant restart filters were replaced more often, independent of the passed fluid volume.

Fluid samples of 1 to 2 liter were collected in sterile Schott Duran glass bottles (Wertheim, Germany).

Sampling was performed once a day in September 2007, April 2008, June 2009, and July 2009. An intense monitoring was done after 23 days of plant downtime in September 2011. During that monitoring, eight fluid samples were initially collected every 15 m^3 after plant restart and finally at an interval of 385 m^3. We particularly focused on samples collected after the exchange of one borehole volume to observe the effects in the filter screens and the near borehole area.

Geochemical and mineralogical analyses

The fluid temperature and pH were determined on-site using a pH/mV/temperature meter (WTW, Weilheim, Germany) during the sampling procedures. Redox potential was measured using an electrode installed in a flow-through chamber (BWG, Neubrandenburg, Germany). The characterization and quantification of the DOC was performed according to Huber and Frimmel (1996) using size-exclusion-chromatography with subsequent ultra violet and infrared detection through a liquid chromatography organic carbon detection (LC–OCD, Toso, Japan) device as described in Vetter et al. (2012).

Fluid-soluble anions and cations, including ion balance, were calculated as shown in Lerm et al. (2013). In the present study, we focused on the ions involved in redox processes relevant for microbial activity present in the geothermally used fluid. The sulfate and iron concentrations were quantified according to DIN EN ISO 17294-2 (E29) and DIN EN ISO 10304-1 (D19) as described in Lerm et al. (2013). The dissolved gas volume was quantified on-site using a mobile degasser (BWG, Neubrandenburg, Germany) and a drum-type gas meter (Ritter, Bochum, Germany), while the gas composition was analyzed using a gas chromatograph with a thermal conductivity detector (TCD) (SHIMADZU, Duisburg, Germany). The gas measurements were carried out according to DIN 1343. The dissolved hydrogen sulfide concentration was determined using an amperometric H_2S micro-sensor (AMT Analysenmesstechnik GmbH, Germany). This method allows for increased sensitivity com-

pared with the methylene blue method, with an accuracy of ± 1% and a lower detection limit of 50 µg l^{-1}.

The sulfur isotopic composition was measured using an NC 2500 elemental analyzer connected to a Thermo Quest Delta+XL mass spectrometer (Thermo Fisher Scientific, Waltham, USA) and is expressed as a delta-notation; $\delta^{34}S=(^{34}S/^{32}S)_{sample}/(^{34}S/^{32}S)_{CDT}-1$. The carbon isotopic composition was determined using a DELTAplusXL mass spectrometer (Thermo Fisher Scientific, Waltham, USA) and is expressed as a delta-notation; $\delta^{13}C= (^{13}C/^{12}C)_{sample}/(^{13}C/^{12}C)_{PDB}-1$.

The particle load in filters from the topside facility was determined using the scale Kern KB 650-2MN (Kern Scales Technic, East Sussex, UK) with an analytical accuracy of 0.01 g. The residues in the filters were analyzed as described in Lerm et al. (2013).

Genetic fingerprinting

Genetic fingerprints of bacterial communities in fluids were performed at AMODIA Bioservice GmbH (Braunschweig, Germany), based on the filtration of 1 liter of fluid using a cellulose acetate filter with a 0.22 µm pore size (Sartorius, Goettingen, Germany), and single-strand conformation polymorphism (SSCP) fingerprinting according to Schwieger and Tebbe (1998). Due to long-term monitoring, genetic profiles were partly generated individually and subsequently arranged. Partial 16S rRNA genes were PCR-amplified by using the universal bacterial primer set F519/ R926-ph (Schwieger and Tebbe 1998).

The SRB community was analyzed through polymerase chain reaction-denaturing gradient gel electrophoresis (PCR-DGGE) (Muyzer et al. 1993) as described in Lerm et al. 2013 using the DCode System (Bio-Rad, Hercules, USA). The sequencing of the reamplified *dsr*B gene fragments was performed at GATC Biotech AG (Konstanz, Germany). The nucleotide sequences obtained after DNA sequencing were analyzed using the ClustalW Multiple alignment tool (Thompson et al. 1994) and the Basic Local Alignment Search Tool (BLAST) of the NCBI database (Altschul et al. 1990) and the Ribosomal Database Project (RDP) Classifier of the RDP database (Wang et al. 2007). Taxonomic assignment was performed by the RDP Classifier and a confidence threshold of 80%. The sequences in this study are available in the NCBI database under the GenBank accession numbers KJ689383 - KJ689423. The sequences deposited under the GenBank accession numbers JQ291339 - JQ291348 were already published in Lerm et al. (2013).

Quantification of Bacteria, SRB, and sulfur-oxidizing Halothiobacillus using real-time PCR

Abundances of Bacteria, SRB, and sulfur-oxidizing *Halothiobacillus* were determined in eight samples collected from the cold well during plant restart in September 2011, after 23 days of downtime, with respect to cumulative produced fluid volume. Quantitative real-time PCR (qPCR) analyses of total 16S rRNA, *dsr*A genes for SRB and specific *Halothiobacillus* 16S rRNA genes were performed using a StepOnePlus^{TM} real-time PCR (Applied Biosystems, Carlsbad, USA). For bacteria, the primer pair Uni331F/Uni797R (Nadkarni et al. 2002) was applied. The cloned full-length 16S rRNA gene of *Escherichia coli* strain JM109 was used as the standard. Total SRB were quantified as described in Lerm et al. (2013) using the primers DSR1F/DSR500R (Wagner et al. 1998, Wilms et al. 2007). *Halothiobacillus* sp. quantification was performed using the primer pair 385F (5´AAA GCA CTT TTA TCG GGG AA 3´) and 555R (5´AGA CTT AAG CTT CCG CCT AC 3´) amplifying a 16S rRNA specific gene fragment. Primers were designed using NCBI Primer BLAST (Ye et al. 2012). The specificity of the primer set was assessed by applying them to the sample material followed by sequencing. The cloned 385F-555R 16S rRNA gene fragment of *Halothiobacillus* sp. (DSMZ 15074) was used as a standard for quantitative analysis. DNA concentration of plasmid and plasmid dilutions from 10^{-1} to 10^{-8} served as the template for the qPCR standard curves.

Each PCR reaction (20 µL) contained 10 µL Power SYBR® Green Master Mix (Life Technologies, Carlsbad, CA, USA), 0.2 µM of each primer, 10 µg BSA, and 1 µL of DNA template. The reaction conditions for amplification of total bacterial, SRB, and *Halothiobacillus* DNA comprised a 10 min initial denaturation step at 95 °C, followed by 35 cycles of amplification with 10 s of denaturation at 95 °C, annealing for 20 s at 60 °C, 58 °C, and 59 °C, respectively, and elongation at 72 °C for 30 s, 30 s, and 20 s, respectively. After each run, a melting curve was gathered between 60 °C, 58 °C, 59 °C, respectively, and 95 °C to distinguish between specific amplicons and unspecific signals. The qPCR amplification factor for the determination of the total bacterial, SRB, and *Halothiobacillus* sp. gene copy number was 1.98, 2.1, and 1.9, respectively. The limit of detection was $9x10^2$ for total bacterial 16S rDNA, $4\ x10^2$ for *Halothiobacillus* specific 16S rDNA, and $2x10^3$ for the *dsr* gene fragments.

Quantitative PCR measurements were done in triplicates. The standard deviations of the replicates were one power of ten lower than the measured value.

Results

Geochemical characteristics of the geothermal fluid

The geochemistry of the fluids produced from the cold and warm well of the geothermal plant was analyzed with respect to relevant microbial parameters including electron donors and acceptors, reflecting the potential activity and abundance of different microbial communities (Table 1).

Table 1: Temperature, pH, ferrous iron concentration and gas content in fluids collected from the cold and warm well during regular operation from 2007 to 2011, shown with standard deviations.

Measurements		T [°C]	pH [-]	Fe^{2+} [mg l^{-1}]	CO_2 [Vol%]	N_2 [Vol%]	H_2S [Vol%]	H_2 [Vol%]	CH_4 [Vol%]
Cold well (CW)	2007	46.3 ± 0.3	6.1 ± 0.2	16.2 ± 0.6	-	-	-	-	-
	2008	47.0 ± 0.0	6.1 ± 1.0	15.0	-	-	-	-	-
	2009	46.9 ± 0.9	6.1 ± 0.1	16.6 ± 1.3	-	-	-	-	-
	2010	47.1 ± 0.5	6.1 ± 0.1	18.4 ± 0.4	-	-	-	-	-
	2011	46.7 ± 0.3	6.1 ± 0.1	21.8 ± 9.3	86.8 ± 0.6	12.8 ± 0.5	0.2 ± 0.03	0.2 ± 0.05	0.02 ± 0.005
	2012	46.7 ± 0.4	6.1 ± 0.0	18.4 ± 3.2	86.0 ± 0.1	13.2 ± 0.5	0.74 ± 0.08	0.003	0.02 ± 0.004
Warm well (WW)	2007	74.2 ± 0.0	5.9 ± 0.0	13.2	-	-	-	-	-
	2008	71.6 ± 0.9	5.9 ± 0.1	13.1 ± 0.4	86.6	13.1	b.d.l.	0.03	0.02
	2009	70.8 ± 5.2	6.0 ± 0.0	14.3 ± 1.9	-	-	-	-	-
	2010	70.8 ± 3.2	6.0 ± 0.1	14.3 ± 1.1	-	-	-	-	-
	2011	76.9 ± 0.8	6.0 ± 0.1	14.7 ± 1.0	83.9	15.9	b.d.l.	0.005	0.019
	2012	76.8 ± 0.6	6.0 ± 0.1	15.4	83.3	16.5	b.d.l.	<0.01	0.024

Oxygen, nitrate and nitrite concentration were below the limit of detection, - not determined

The salinity of the geothermal fluids was determined as 130 g l^{-1} and classified as high and of the Na-Cl type, with a pH of 6. The redox potentials (standard hydrogen electrode, SHE) in fluids produced from the warm and the cold well reflected reducing conditions, with values ranging from 1 to -60 mV depending on the operation mode. Concentrations of potential electron acceptors such as SO_4^{2-} and electron donors such as Fe^{2+}, HS^-, and H_2 differed between fluids from the warm and the cold well, whereas CO_2 concentrations (86 Vol%) and DOC values (3.5 mg C l^{-1}(Vetter et al. 2012)) were in the same range during regular operation. The sulfate concentration in fluids from the cold well was 912 mg l^{-1} on average and was approximately 8% lower compared with fluids produced from the warm well (Fig. 1). Oxygen, nitrate and nitrite concentrations were below the limit of detection.

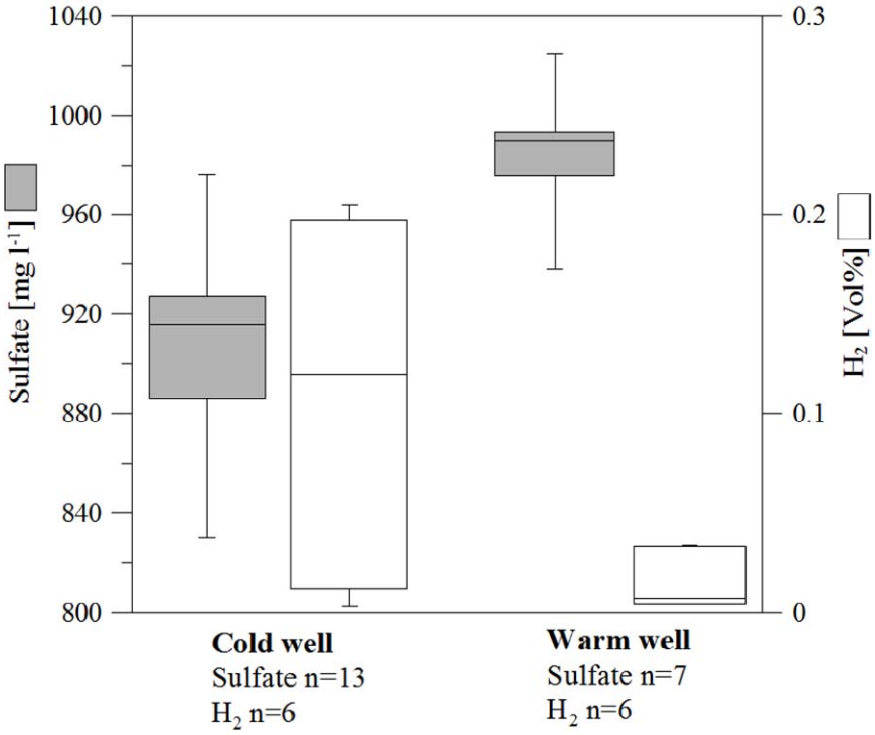

Fig. 1: Box plot diagram of sulfate and hydrogen concentrations in the fluids produced from the cold well and the warm well during regular operation from 2007 to 2011. The sulfate values were directly measured after changing the operation mode, and the fluid flow direction was excluded.

Average concentrations of ferrous iron and hydrogen sulfide were higher in the cold fluids (Fe^{2+} 17.9 mg l^{-1}, H_2S 0.41 Vol%) compared with warm fluids (Fe^{2+} 14.7 mg l^{-1}, H_2S below detection limit). The total gas content was 76 ml l^{-1} on the cold side and 75 ml l^{-1} on the warm side. Traces of methane (CH_4) were detected in the cold and the warm fluids at a concentration of 0.02 Vol%. The total hydrocarbon content was below 0.001 ml l^{-1}.

The isotopic signature of $\delta^{34}S$ in fluids produced from the warm well in September 2011 was 32.1 ‰ CDT, and that for fluids produced from the cold well in August 2010 was 32.2 ‰ CDT. Mineral scales collected from filter bags during regular operation revealed $\delta^{34}S$ values between 8 ‰ CDT and 12 ‰ CDT. In contrast, FeS minerals sampled from a filter bag after 23 days of a downtime phase in September 2011 showed a two-fold higher $\delta^{34}S$ value of 25 ‰ CDT. The carbon isotopic signature of the calcites $d^{13}C_{CO2}$ differed between the warm well (-10 ‰ PDB) and the cold well (-13 ‰ PDB).

To investigate the effects of plant downtime, the SO_4^{2-} - S^{2-} - H_2S system was studied in detail in September 2011. Relevant microbial parameters of the fluids produced from the cold well at production of one borehole volume (<35 m^3) and fluid production from the reservoir (> 35 m^3) are shown in figure 2. At the beginning of the recharge mode in September 2011 and before plant downtime, the H_2S concentration was 220 µg l^{-1}. In addition, the ferrous iron

concentration was 33 mg l^{-1} and the sulfate concentration was approximately 980 mg l^{-1}. After 23 days of plant downtime, the H_2S concentration was 375 µg l^{-1} after producing approximately 10 m^3 of fluid. This value decreased significantly to 180 µg l^{-1} within one day, after producing 510 m^3 of fluid. A similar trend was observed for the sulfate concentration, showing a maximum of 1,600 mg l^{-1}, followed by a decreased after production of 510 m^3 of fluid to 980 mg l^{-1}. The ferrous iron concentration was 22 mg l^{-1} at the beginning of the restart and decreased to 17 mg l^{-1} with ongoing fluid production. Additionally, increased DOC values of up to 98.8 mg C l^{-1} were observed in the fluids collected immediately after restart and subsequently decreased to values observed during regular operation (DOC 3.5 mg C l^{-1}) after the production of one borehole volume. Volatile fatty acids like acetate were only barely detected after plant restart (data not shown). Temperature (45.4 °C ± 0.8) and pH (6.2 ± 0.07) stayed in a similar range during restart.

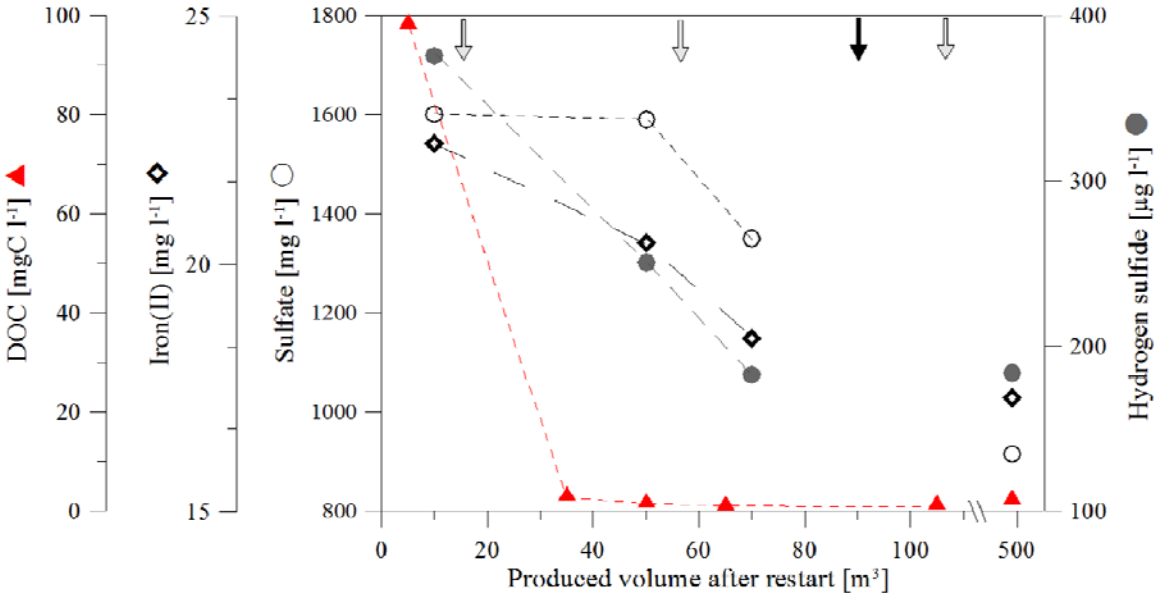

Fig 2: Sulfate, ferrous iron, hydrogen sulfide, and DOC concentrations determined in fluids collected from the cold well during plant restart in September 2011. One borehole volume amounts to 35 m^3. ⇩ Short stop of operation (<3 h). ↓ 19 hour stop of operation.

Quantification and characterization of scales in filters

The particle load in the fluids was calculated based on the amount of scales collected in filters of the topside facility in reference to the fluid volume produced. The particle load in the fluids varied during the recharge mode and regular plant operation. At the beginning of the recharge mode in 2009, 2010, and 2011, the particle load was between 1,000 and 9,000 g m^{-3} and con-

tinuously decreased to 0.01 g m^{-3} during the production of approximately 14,000 m^3 of fluid (Fig. 3). In contrast, after plant downtime in September 2011 and subsequent restart, the particle load was 50,000 g m^{-3}. During the further production of 80,000 m^3 fluid, the particle load decreased to 0.01 g m^{-3}.

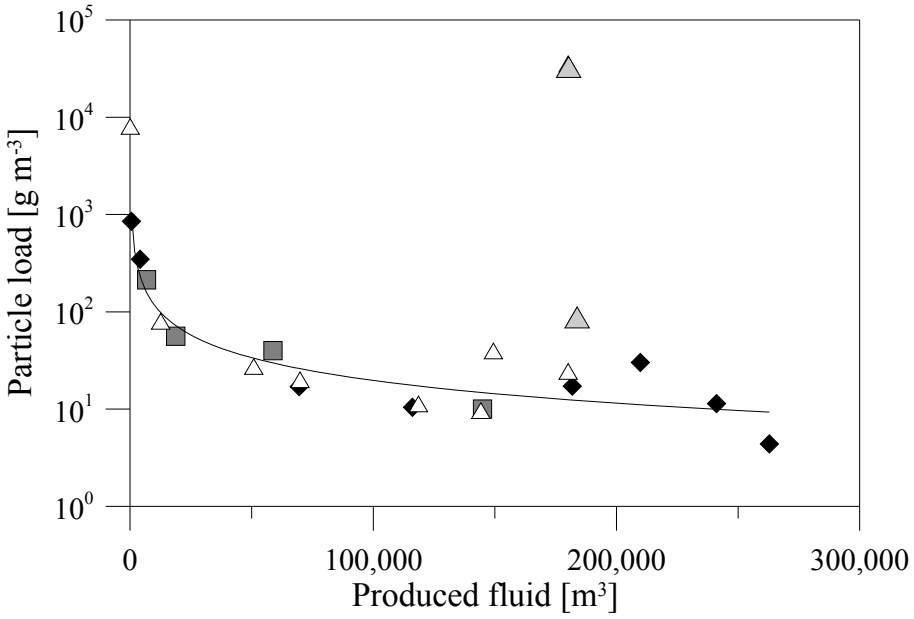

Fig. 3: Particle loading rate in filters installed in the topside facility of the geothermal plant during the charge mode in 2009 (◆), 2010 (■), 2011(△) and at the plant restart after the 23 day downtime period in 2011 (▲).

During regular plant operation and fluid production from the warm well, the majority (80%) of mineral precipitates in filters comprised calcium carbonate crusts and thin iron sulfide crusts. After heat extraction to temperatures of approximately 46 °C, the mineral precipitates accumulated in filters before reinjection were predominantly crusts of iron sulfide (FeS). FeS was also the main mineral residue (~ 90%) in filters during recharge mode before and after heat extraction. The mineral phases in filters during regular plant operation have been previously described (Lerm et al. 2013).

After a downtime of 23 days and fluid production from the cold well, the mineral precipitates mainly consisted of black, fine-grained particles of FeS (97%) (Fig. 4). The rough particles in these filters comprised FeS-scales and reservoir materials, such as quartz, clay, and $CaCO_3$.

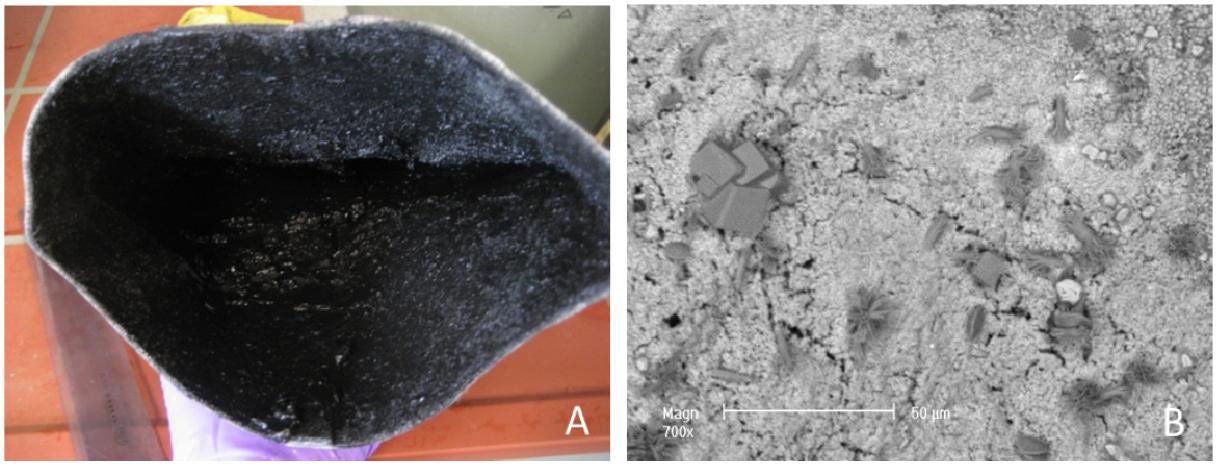

Fig. 4: Mineral scales in the filters at the topside facility in Neubrandenburg collected in September 2011, (A) increased amounts of black, fine grained particles in a filter, (B) back-scatter picture of iron sulfide scales with growing $CaCO_3$ crystals.

Microbial communities in geothermal fluids during regular operation and restart events after plant downtimes

From September 2007 to July 2009, SSCP analyses revealed complex microbial communities in fluids collected from the cold well, during regular operation and subsequent to plant downtimes. The SSCP profiles differed in the abundance and intensity of bands (Fig. 5). Two plant downtime events, lasting six days (April 2008) and three months (June 2009), led to a different banding pattern with a higher microbial diversity.

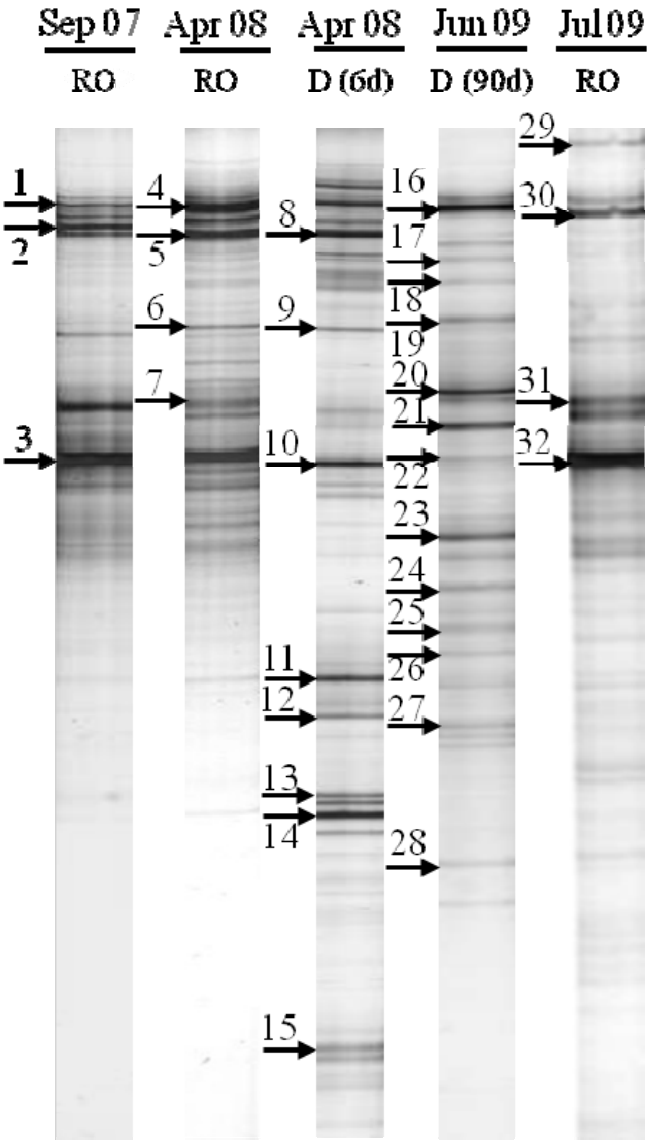

Fig. 5: SSCP analysis of bacterial 16S rRNA gene fragments using DNA extracted from fluids produced from the cold well from September 2007 until July 2009. RO: Regular Operation, D: Downtime (duration [d]). The arrows indicate the positions of sequenced bands. (SSCP profiles retrieved from fluids collected in September 2007, April 2008, and July 2009 were previously published in Lerm et al. 2013).

The fluids produced from the cold well during regular operation (September 2007, April 2008, and July 2009) contained organisms affiliated with the phylum *Firmicutes* and classes of Beta-, Delta-*Proteobacteria* (Fig. 5, Table 2).

Table 2: Closest relative of partial bacterial 16S rRNA gene sequences and GenBank accession numbers retrieved from SSCP-profiles of fluids collected from the cold well during regular plant operation and after downtime phases

Plant Operation	Sample	Band	Class	Closest relative, (Genbank accession number)	Similarity [%]	GenBank Accession Number
Regular operation	Sep 07	1	Delta-*Proteobacteria*	*Desulfohalobium utahense,* strain EtOH3 (DQ067421)	98	JQ291339
		2	Delta-*Proteobacteria*	Uncultured *Desulfohalobiaceae* bacterium, clone J2Dbac (DQ386183)	98	JQ291340
		3	*Firmicutes*	*Desulfotomaculum* sp., strain NA401 (AJ866942)	90	JQ291341
Regular operation	Apr 08	4	Delta-*Proteobacteria*	*Desulfohalobium utahense,* strain EtOH3 (DQ067421)	98	JQ291342
		5	*Firmicutes*	Candidatus *Desulforudis audaxviator* MP104C (NR_075067)	96	JQ291343
		6	*Firmicutes*	Uncultured *Halanaerobiaceae* bacterium, clone L5Dbac (DQ386209)	95	JQ291344
		7	*Firmicutes*	*Desulfotomaculum* sp., strain NA401 (AJ866942)	90	JQ291345
After downtime (6 days)	Apr 08	8	*Firmicutes*	Candidatus *Desulforudis audaxviator* strain MP104C (NR_075067)	96	KJ689403
		9	*Firmicutes*	Uncultured *Halanaerobiaceae* bacterium, clone L5Dbac (DQ386209)	95	KJ689404
		10	*Firmicutes*	*Desulfotomaculum* sp., strain NA401 (AJ866942)	90	KJ689405
		11	Gamma-*Proteobacteria*	*Thiomicrospira* sp. L-12 (AF064544)	97	KJ689406
		12	Gamma-*Proteobacteria*	*Thiomicrospira crunogena* XCL-2, (CP000109)	98	KJ689407
		13, 14	Gamma-*Proteobacteria*	*Halothiobacillus sp.* HL7 (KC017786)	98, 99	KJ689408, KJ689409
		15	Epsilon-*Proteobacteria*	Uncultured *Sulfuricurvum* sp. RIFRC-1 (CP003920)	98	KJ689410
After downtime (90 days)	Jun 09	16	Delta-*Proteobacteria*	*Desulfohalobium utahense,* strain EtOH3 (NR_043521)	98	KJ689411
		17	*Firmicutes*	Candidatus *Desulforudis audaxviator,* strain MP104C (NR_075067)	96	KJ689412
		18	*Firmicutes*	Uncultured *Halanaerobium* sp., clone AS-P4-Sed-48 (FM879114)	99	KJ689413
		19	*Firmicutes*	Uncultured *Clostridia* bacterium clone b18-223 (JX576041)	90	KJ689414
		20	*Firmicutes*	Uncultured *Halothermothrix* sp., clone RS39 (HQ397382)	98	KJ689415
		21, 23	*Firmicutes*	*Desulfotomaculum* sp. NA401, strain NA401 (AJ866942)	90, 86	KJ689416
		22	*Thermotogae*	*Thermotogales* bacterium PhosAc3 (FN611033)	91	KJ689417, KJ689418
		24, 28	*Bacteroidetes*	Uncultured *Anaerophaga* sp., clone TCB200x (DQ647171)	99, 98	KJ689419, KJ689423
		25	*Firmicutes*	*Halanaerobium* sp. L21-Ace-D5 (KC631810)	98	KJ689420
		26	*Firmicutes*	*Halanaerobiaceae* bacterium Benzl(DQ386220)	98	KJ689421
		27	*Firmicutes*	*Desulfotomaculum* sp. TGB60-1 (JX183068)	94	KJ689422
Regular operation	Jul 09	29	Beta-*Proteobacteria*	*Comamonas sp.* MZ_15 (JF690938)	100	JQ291346
		30	Delta-*Proteobacteria*	*Desulfohalobium utahense* , strain EtOH3 (DQ067421)	98	JQ291347
		31, 32	*Firmicutes*	*Desulfotomaculum* sp. NA401, strain NA401 (AJ866942)	90, 90	JQ291345, JQ291348

Specifically, the genetic profile of fluids showed bands whose sequences were affiliated with *Comamonas* sp. (band 29), fermentative *Halanaerobiaceae* (band 6) as well as several SRB, such as *Desulfotomaculum* sp. (bands 3, 7, 31, 32), Candidatus *Desulforudis audaxviator* (band 5), and *Desulfohalobium* (bands 1, 2, 4, 30). Consistently, *dsr* gene-based fingerprinting specific for SRB also revealed sequences related to the family of *Desulfohalobiaceae* and the genus *Desulfotomaculum*.

After six days of plant downtime (April 2008), additional bands appeared in the genetic profile whose sequences were affiliated with the sulfur-oxidizing genera *Thiomicrospira* (bands 11, 12), *Halothiobacillus* (bands 13, 14), and *Sulfuricurvum* (band 15). After three months of plant downtime, in June 2009, additional sequences affiliated with *Halothermothrix* (band 20), *Anaerophaga* (bands 24, 28), *Thermoactinomycetaceae* (band 19), and *Thermotogales* (band 22) were detected.

Intense monitoring - Microbial composition in fluids produced after plant downtimes in September 2011

The microbial community of fluids produced from the cold well immediately after 23 days of plant downtime in September 2011 contained *Clostridia,* Delta- and Gamma- *Proteobacteria*, *Bacteroidia*, and *Synergistia* with sequences affiliated with *Halanaerobacteriaceae*, the genera *Desulfotomaculum, Halothiobacillus, Anaerophaga*, and *Thermovirga* (Fig. 6, Table 3).

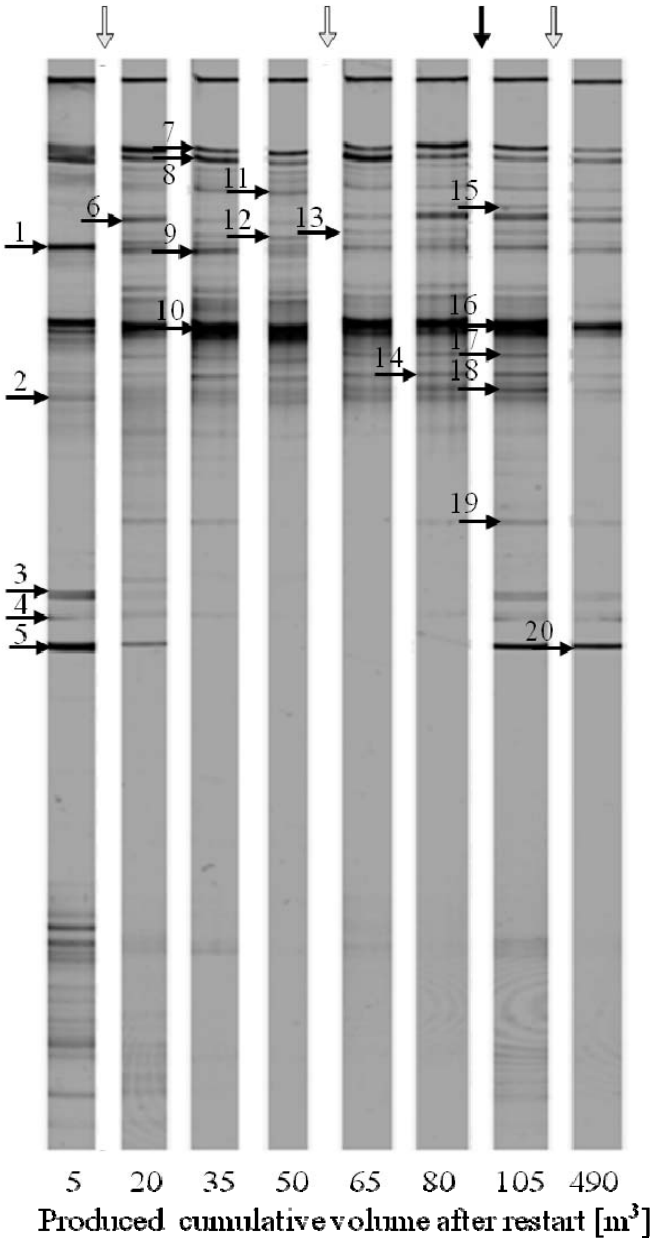

Fig. 6: SSCP analysis of bacterial 16S rRNA gene fragments using DNA extracted from the fluids produced from the cold well after plant restart in September 2011 with respect to time and produced fluid volume after restart. The arrows indicate the positions of the sequenced bands. ⇩ Short stop of operation (<3 h). ↓ 19 hour lasting stop of operation.

Table 3: Closest relative of partial bacterial 16S rRNA gene sequences and GenBank accession numbers retrieved from SSCP-profiles of fluids collected from the cold well after plant restart in September 2011.

Band	Class	Closest relative, (Genbank accession number)	Similarity [%]	GenBank Accession Number
1	*Clostridia*	Uncultured *Halanaerobiaceae* bacterium, clone L5Dbac (DQ386209)	96	KJ689383
2	*Clostridia*	*Desulfotomaculum* sp. Mechichi-2001 (AY069974)	90	KJ689384
3-5	Gamma-*Proteobacteria*	*Halothiobacillus* sp. HL7 (KC017786)	99, 99, 100	KJ689385-KJ689387
6	*Synergistia*	Uncultured *Thermovirga* sp., clone TCB169x (DQ647105)	98	KJ689388
7	Delta-*Proteobacteria*	*Desulfohalobium utahense* strain EtOH3 (NR_043521)	98	KJ689389
8	Delta-*Proteobacteria*	Uncultured *Desulfohalobiaceae* bacterium, clone J2Dbac (DQ386183)	99	KJ689390
9	*Clostridia*	Uncultured *Halanaerobiaceae* bacterium, clone L5Dbac (DQ386209)	96	KJ689391
10	*Clostridia*	*Desulfotomaculum* sp. NA401 (AJ866942)	91	KJ689392
11,12	*Clostridia*	*Halothermothrix orenii* H 168 (NR_074915)	93, 93	KJ689393, KJ689394
13	*Clostridia*	*Halothermothrix orenii* H 168 (NR_074915)	90	KJ689395
14	*Clostridia*	*Halanaerobium* sp. S191 (FJ858788)	99	KJ689396
15	*Clostridia*	Uncultured *Halanaerobiaceae* bacterium, clone L5Dbac (DQ386209)	96	KJ689397
16, 17	*Clostridia*	*Desulfotomaculum* sp. NA401 (AJ866942)	91, 91	KJ689398, KJ689399
18, 19	*Bacteroidetes*	Uncultured *Anaerophaga* sp., clone TCB200x (DQ647171)	92, 96	KJ6899400, KJ689401
20	Gamma-*Proteobacteria*	*Halothiobacillus* sp. HL7 (KC017786)	99	KJ689402

Sequences related to *Desulfotomaculum* (bands 10, 16, 17), *Desulfohalobium* sp. (band 7), *Halothermothrix* sp. (bands 11, 12, 13), and *Halanaerobium* (band 14), were present in all fluids, indicated as bands at the same position in the genetic profiles, resulting in a similar banding pattern, and the bands showed partial differences in intensities.

Sulfur-oxidizing *Halothiobacillus* related species (bands 3, 4, 5) disappeared after the produced cumulative volume exceeded 20 m^3. Short stops during restart (< 3 h) did not increase the band intensity of these species, whereas a 19-hour stop correlated with their re-appearance (band 20). Similar observations, but to a lesser extent, were obtained for *Halanaerobacteriaceae* (band 1) and *Anaerophaga* species (band 19), also showing a decrease in intensities with ongoing fluid production, but no changes were observed after short stops. Corresponding to the analyses of the total bacterial community, the SRB specific fingerprinting revealed sequences affiliated with the family of *Desulfohalobiaceae* and the genus *Desulfotomaculum* in all fluids.

Intense monitoring - Quantification of Bacteria*, SRB, and relatives of* Halothiobacillus *in fluids produced during plant restart in September 2011*

Total DNA, total bacterial 16S rRNA, *dsr*A, and *Halothiobacillus* sp. specific 16S rRNA gene copies were calculated as a quantitative measure of total biomass, to determine the abundance of *Bacteria*, SRB, and *Halothiobacillus* in the cold well during restart after 23 days of plant downtime in September 2011 (Fig. 7).

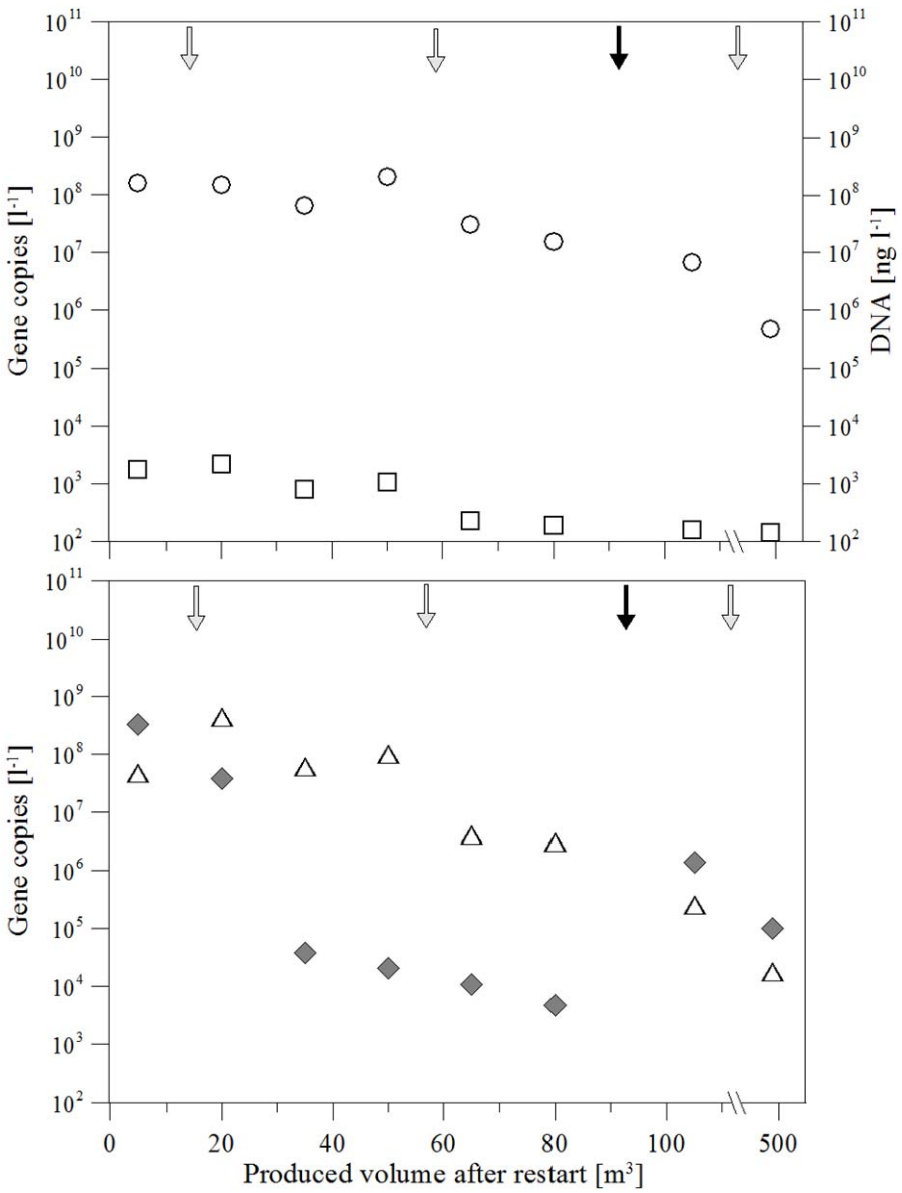

Fig. 7: (A) □ Total DNA concentration and total abundance of *Bacteria*, (B) SRB, and *Halothiobacillus* sp., based on the ○ 16S rRNA, △ *dsr*A, and ◆ specific 16S rRNA gene fragments, respectively, in fluids collected from the cold well after plant restart in September 2011 (23 d downtime) with respect to cumulative produced fluid volume after restart. ⇩ Short stop of operation (<3 h). ↓ 19 hour lasting stop of operation.

Halothiobacillus sp. abundance was included in the analyses, as this species was detected in the fluids directly collected after the initial plant restart and after the 19-hour stop during the restart event shown by genetic fingerprinting.

Bacterial 16S rRNA and *dsr*A gene copy number decreased with the cumulative produced volume. At the beginning, 16S rRNA gene copies l^{-1} was $1x10^9$ and varied during the production of 50 m^3 of fluid from $4x10^9$, $6.5x10^7$, and $2.6x10^8$ copies l^{-1}, respectively. With ongoing fluid production, 16S rRNA gene copy number finally decreased to $4.8x10^5$ at 490 m^3. The

SRB abundance in the first fluid produced after the downtime was $7x10^7$ *dsr*A gene copies l^{-1}. While producing up to 50 m^3 of fluid, *dsr*A gene copy number varied between $6.2x10^7$ and $4.4x10^8$. Subsequently, *dsr*A gene copy number decreased to $1.8x10^4$ after 490 m^3 fluid had been produced. Numbers of *Halothiobacillus* specific 16S rRNA gene copies decreased after plant restart from $3.3x10^8$ to $4.7x10^3$ corresponding to the production of 80 m^3 of fluid. The short operational shut-down phases showed no effect on gene copy number, contrary to the longer shut down phase. The 19-hour stop correlated with an increase in *Halothiobacillus*-specific gene copy numbers, again ranging up to $1.4x10^6$ after production of 25 m^3 from the intermediate restart or 105 m^3 in total. With ongoing fluid production, *Halothiobacillus*-specific gene copy number decreased again to $1x10^5$ after 490 m^3, indicating a slower discharge than observed after the initial restart.

Discussion

Microorganisms in the highly saline fluid of the geothermal heat store

We analyzed regular plant operation and in particular the effects of plant downtimes on the microbial community composition in the cold well of the geothermal heat store. Fluid samples collected before and after downtime phases revealed sequences affiliated with phyla typically described for habitats such as saline lakes and sediments (Jakobsen et al. 2006; Kjeldsen et al. 2007; Mavromatis et al. 2009; Tourova et al. 2013), high-temperature oil fields (Dahle et al. 2008; Sette et al. 2007), and fracture water from a gold mine (Chivian et al. 2008).

As observed in a previous study (Lerm et al. 2013), 16S rRNA sequences affiliated with different SRB (*Desulfohalobium* sp., *Desulfotomaculum* sp., Candidatus *Desulforudis audaxviator*) and relatives of fermentative *Halanaerobiaceae* were detected in the 46 °C fluids produced from the cold well during regular plant operation. Consistently, the detection of *dsr*A gene sequences affiliated with *Desulfohalobiaceae* and species distantly related to *Desulfotomaculum* corroborated the finding that these species dominated the SRB community. During regular operation, this microbial composition of SRB and fermentative bacteria was characteristic for the cold well affected by intense corrosion of the metallic installations. Furthermore, the community composition differed from that of fluids produced from the warm well and the cooled re-injected fluid (Lerm et al. 2013). The physiological characteristics of detected SRB and fermentative bacteria corresponded to the aquifer conditions with respect to temperature, salt concentration, and pH. The lower carbon isotopic signature of the precipitated calcite ($d^{13}C_{CO2}$ -13 ‰ PDB) reflected the higher microbial activity in cold fluids and the degradation of organic substances to CO_2. The abundance of SRB in cold fluids indi-

cated by the genetic fingerprinting and *dsr*A genes correlated to an 8% lower sulfate concentration. Based on the age curve of marine sulfates in geothermal fluids, $\delta^{34}S$ values of 13-18 ‰ CDT would be expected without microbial activity (Holser 1977). Thus, the isotopic signature in the fluids of above 32 ‰ CDT indicated microbial turnover of sulfur components in the fluids. Due to the long-term operation of seven years, the alternating fluid flow direction, and the seasonally dependent longer charging period, the change in the isotopic signature was observed at both sides of the heat store, although higher sulfide content and the abundance of SRB were observed at the cold well only.

Effects of plant downtimes

The results of the present study demonstrate that plant downtimes influence the microbial composition, whereby shifts in the microbial biocenosis were dependent on the duration of downtime. A 23 days downtime, led to an increase of the bacterial 16S rDNA and *dsr*A gene copy number by a factor of 10^3 and 10^4, respectively, compared to numbers detected during regular operation. The specific 16S rRNA gene copy number of the sulfur-oxidizing chemolithoautotroph *Halothiobacillus* even increased by a factor of 10^5 in consequence of plant downtime.

These findings indicated an increase in the microbial abundance in fluids produced from the cold well directly after the downtime phase. Improved growth conditions probably led to an accelerated growth of microorganisms, specifically SOB. In addition, the lack of removal of microbial cells by the fluid flow during stagnant conditions resulted in a higher microbial abundance after plant downtime phases. This result is consistent with the findings of Van Beek (1989) who showed that clogging caused by microorganisms and mineral precipitates can be slowed down through continuous fluid production in water systems and groundwater wells as microbes and scales will be continuously removed. Whether microbial activity in the cold well is associated with the sporadically 28-fold higher DOC concentration in the fluid subsequent to plant downtime is not clear. Nevertheless, microbial metabolic processes were likely triggered through corrosion products, as corrosion of the well casing and the submersible pump supplied energy to the system during plant downtime.

Enhanced corrosion processes during the downtime phase were indicated by the higher abundance of SRB and SOB in fluids produced after plant restart. An enrichment of hydrogenotrophic SRB, such as *Desulfotomaculum* species reflected the increased availability of hydrogen. In addition, chemoheterotrophic sulfate reduction could have been favored through the enhanced availability of organic acids produced by co-existing fermentative bac-

teria showing a higher diversity and abundance during downtime phases. However, volatile fatty acids like acetate were barely detected after plant restart. The enrichment of SOB likely had an important effect on corrosion. SOB metabolism produces sulfuric acid through either sulfur or sulfide oxidation; thus, SOB are often involved in the enhanced corrosion of steel (Javaherdashti 2008). Changes in pH and temperature, as decisive factors for shifts in microbial community composition, could not be detected in the fluids produced after plant downtime, probably due to the high flow rate. However, temperature changes could have occurred in the topside facility and wellbore during plant downtime, becoming particularly relevant during long-term downtimes of more than 19 hours, likely favoring the growth of microbes.

After the six days of plant downtime, SRB, fermentative *Halanaerobiaceae* and sequences affiliated with the sulfur-oxidizing genera of *Thiomicrospira, Halothiobacillus,* and *Sulfuricurvum* were detected in the fluids produced from the cold well. Organisms belonging to these genera have been isolated from various hypersaline habitats, including lakes and shallow and deep-sea hydrothermal environments (Ruby and Jannasch 1982; Takai et al. 2004; Sorokin et al. 2006; Sievert et al. 2000), lake sediments (Nelson et al. 2007), sulfidic caves, and springs (Porter and Engel, 2008) as well as an underground crude-oil storage cavity (Kodama and Wantanabe 2004). Sequences affiliated to *Sulfuricurvum* were also observed in a shallow low mineralized aquifer in the North German Basin used for subsurface cold storage (Lerm et al. 2011a).

The abundance of strictly aerobic and facultative anaerobic SOB suggested oxygen ingress in the wellbore during plant downtime, although the wells and the topside facility were maintained under pressure during regular plant operation (5 to10 bar) and downtime phases (2 bar) to prevent the precipitation of iron oxides or hydroxides and carbonate minerals due to degassing processes and oxygen ingress. However, after plant shut down the hanging water column in the production tubing caused an absolute pressure near 0.2 bar in the tubing itself and the near wellhead installations until pressure was manually recovered. Until the pressure recovery, it is presumed that oxygen was drawn into the system through leaking equipment and diffused via the wellbore into the anoxic system.

The 5,000,000-fold increased particle load dominated by iron sulfides indicated SRB activity and the enrichment of microbial products due to the stagnant well conditions during downtime. Plant downtime affected also the isotopic composition of sulfur ($^{34}S/^{32}S$) in mineral scales as a result of microbial conversion of sulfur compounds. Iron sulfide minerals sampled from a filter bag after the 23 days downtime phase showed a $\delta^{34}S$ value of 25 ‰ CDT, a twofold higher isotopic signature compared with mineral scales obtained during regular opera-

tion. This result highlights the microbial contribution to scale formation. In addition to the increased mineral content in fluids produced after stagnant phases, the re-suspension of solids was enhanced, reflecting the presence of microbial metabolites, such as sulfuric acid from SOB metabolism, as indicated by the slightly increased ferrous iron concentration in the first fluids produced after downtimes.

Immediately after restart, the hydrogen sulfide concentration in fluids was high and then decreased within the production of two borehole volumes to values similar to those during regular operation, demonstrating potential corrosion activity in the well during stagnant conditions. Moreover, elevated sulfate concentrations at the beginning of the restart process indicated the activity of SOB in the wellbore. To facilitate the effective exchange of sulfur compounds, SOB and SRB are likely associated in biofilms, generating redox conditions suitable for both metabolic pathways. The oxygen ingress during plant downtime did not prevent the growth of SRB, as the oxygen consumption of SOB retained anoxic micro-niches (Dillon et al. 2011). Gamma-*Proteobacteria,* which comprise the genera *Halothiobacillus* and *Thiomicrospira,* are known to co-exist with SRB in biofilms and were additionally linked to corrosion processes of metal surfaces (Kjellerup et al. 2003). Analyses of biofilm structures formed on coupons of mild and stainless steel, which were exposed to the geothermal fluid under plant operation conditions (Würdemann et al. 2014) corroborated the findings of an ongoing biofilm formation on the metallic plant components. Synthrophic SRB and SOB were found to be present within the biofilms (unpublished data). The density of biofilms is dependent on the hydrodynamic conditions during formation and maturation. In simulated drinking water systems biofilms showed a lower density, when the shear stress decreased (Paul et al. 2012).

Intense monitoring after plant downtime - discharge of SOB and SRB

After the 23 days of plant downtime, the sequences affiliated with sulfur-oxidizing *Halothiobacillus* species were detected through genetic fingerprinting until one borehole volume was produced. Correspondingly, qPCR revealed the fast decrease of *Halothiobacillus* specific gene copy numbers by a factor of 10^5. The rapid disappearance of *Halothiobacillus* indicated that these organisms were primarily associated with wellbore fluids and the upper part of the wellbore. Consistently, no SOB were observed through genetic fingerprinting after fluid production of 10 borehole volumes after a three month downtime phase.

In contrast to the rapid decline of SOB, the abundance of SRB decreased much slower with increasing fluid production, as the gene copy number of SRB was only reduced by half after

the production of 14 borehole volumes, indicating that SRB were much more widespread in the well and the reservoir than SOB. Consistently, the fraction of SRB of the total *Bacteria* remained in a more similar range, while the SOB fraction rapidly decreased. A subsequent plant downtime lasting 19 hours correlated with a second increase of *Halothiobacillus* specific gene copies, while three shut down phases of less than three hours showed no enrichment. Hence, short-term downtimes had no visible effect. This effect likely reflects the growth rates of the *Halothiobacillus* representatives. Moreover, no increase was observed for SRB subsequent to less than 19-hour downtime phases, suggesting that the effects were primarily associated with the upper wellbore favoring the growth of SOB, whereas SRB abundance was affected only after even longer plant downtime phases lasting several days. Interestingly, the fluid volume necessary to discharge the SOB was 8 times higher after the 19-hour downtime compared with the restart after 23 days of downtime. It is suggested that the differences in the fluid production rate during restart that had caused varying flow turbulences and thus led to different rates of biofilm detachment before returning to levels of regular operation (Choi and Morgenroth 2003).

In summary, oxygen ingress during stagnant conditions favored microbial abundance and diversity in the cold well as indicated by chemical and biological parameters. Additionally, the oxygen ingress might have enhanced corrosion processes triggered by biofilms. Increased concentrations of corrosion and precipitation products resulting from processes mediated through SRB and SOB, such as iron sulfides, hydrogen sulfide, and sulfate and an altered sulfuric isotopic signature of precipitates and scales provided evidence for microbial activity and the microbial influence on scale formation, respectively. The abundance of SOB in the highly reduced system indicated corrosion-enhancing oxygen ingress into the well when the pressure was below ambient air pressure immediately after the shut-down of the pump. The increase of SOB during downtime and the fast decline after plant restart can be regarded as an evidence for the exclusive effect on the upper wellbore. To minimize corrosion and precipitation processes due to oxygen-dependent SOB growth, technical adjustments are required to reduce plant downtimes and sufficiently maintain the pressure in the geothermal plant.

Acknowledgments

The authors would like to thank the public utilities of the city of Neubrandenburg for providing access to the topside facility of the geothermal heat store. In addition, the authors would also like to thank AMODIA Bioservice GmbH (Braunschweig, Germany) for SSCP analyses and to Dr. Alexandra Vetter and Dr. Andrea Vieth-Hillebrand for the DOC measurements and

Dr. Birgit Plessen, from GFZ German Research Centre for Geoscience, for the determination of the carbon isotopic composition. Moreover, the authors would like to thank Dr. Heinrich Taubald from the Department of Geosciences of Tübingen University for the sulfur isotopic composition measurements.

Ethical Statement

This work was supported by Federal Ministry of the Environment, Natural Conservation and Nuclear Safety (BMU, grant No. 0327634). The authors declare that they have no conflict of interest. This article does not contain any studies with human participants or animals performed by any of the authors.

References

Altschul S, Gish W, Miller W (1990) Basic local alignment search tool. J Mol Biol 215:403–410.

Amend J, Teske A (2005) Expanding frontiers in deep subsurface microbiology. Palaeogeogr Palaeoclimatol Palaeoecol 219:131–155.

Bauer S, Beyer C, Dethlefsen F, Dietrich P, Duttmann R, Ebert M, Feeser V, Görke U, Köber R, Kolditz O, Rabbel W, Schanz T, Schäfer D, Würdemann H, Dahmke A (2013) Impacts of the use of the geological subsurface for energy storage: an investigation concept. Environ Earth Sci 70:3935–3943.

Chivian D, Brodie EL, Alm EJ, Culley DE, Dehal PS, Desantis TZ, Gihring TM, Lapidus A, Lin L, Lowry SR, Moser DP, Richardson PM, Southam G, Wanger G, Pratt LM, Andersen GL, Hazen TC, Brockman FJ, Arkin AP, Onstott TC (2008) Environmental genomics reveals a single-species ecosystem deep within earth. Science 322:275–278.

Choi YC, Morgenroth E (2003) Monitoring biofilm detachment under dynamic changes in shear stress using laser-based particle size analysis and mass fractionation. Water Sci Technol 47:69–76.Corsi R (1986) Scaling and corrosion in geothermal equipment: problems and preventive measures. Geothermics 15:839–856.

Dahle H, Garshol F, Madsen M, Birkeland N-K (2008) Microbial community structure analysis of produced water from a high-temperature North Sea oil-field. Antonie van Leeuwenhoek 93:37–49.

Dillon JG (2011) The role of sulfate reduction in stromatolites and microbial mats: ancient and modern perspectives. In: Tewari V, Seckbach J (eds) STROMATOLITES Interaction Microbes with Sediments. Springer Netherlands, Dordrecht 571–590.

DIN 1343 (1990) -01 Reference conditions, normal conditions, normal value; Concepts and values.

DIN EN ISO 17294-2 (2005) -02 German standard methods for the examination of water, waste water and sludge - Cations (group E) - Part 29: Determination of 61 elements by inductively coupled plasma mass spectrometry (ICP-MS) (E 29).

DIN EN ISO 10304-1 (2009) -07 Water quality - Determination of dissolved anions by liquid chromatography of ions - Part 1: Determination of bromide, chloride, fluoride, nitrate, nitrite, phosphate and sulfate (ISO 10304-1:2007).

Enning D, Garrelfs J (2014) Corrosion of iron by sulfate-reducing bacteria: new views of an old problem. Appl Environ Microbiol 80:1226–36.

Fichter C, Falcone G, Reinicke KM, Teodoriu C (2011) Probabilistic analysis of failure risk in the primary geothermal cycle. Thirty-Sixth Workshop on Geothermal Reservoir Engineering Stanford University, California.

Gallup DL (2009) Production engineering in geothermal technology: A review. Geothermics 38:326–334.

Griebler C, Lueders T (2009) Microbial biodiversity in groundwater ecosystems. Freshw Biol 54:649–677.

Hamilton WA (1985) Sulphate-reducing bacteria and anaerobic corrosion. Annu Rev Microbiol 39:195–217.

Holser W (1977) Catastrophic chemical events in the history of the ocean. Nature 267:403–408.

Houben GJ, Weihe U (2010) Spatial distribution of incrustations around a water well after 38 years of use. Groundwater 48:53–58.

Howsam P (1988) Biofouling in wells and aquifers. Water Environ J 2:209–215.

Huber S, Frimmel F (1996) Size-exclusion chromatography with organic carbon detection (LC-OCD): a fast and reliable method for the characterization of hydrophilic organic matter. Vom Wasser 86:277–290.

Javaherdashti R (2008) Microbiologically influenced corrosion: an engineering insight. Springer, London.

Javaherdashti R (2011) Impact of sulphate-reducing bacteria on the performance of engineering materials. Appl Microbiol Biotechnol 91:1507–17.

Kabus F, Wolfgramm M (2009) Aquifer thermal energy storage in Neubrandenburg - monitoring throughout three years of regular operation. Proc. of the 11th Intern. Conf. on Energy Storage. Stockholm, Sweden.

Kjeldsen KU, Loy A, Jakobsen TF, Thomsen TR, Wagner M, Ingvorsen K (2007) Diversity of sulfate-reducing bacteria from an extreme hypersaline sediment, Great Salt Lake (Utah). FEMS Microbiol Ecol 60:287–98.

Kjellerup B V, Olesen BH, Nielsen JL, Frolund B, Odum S, Nielsen PH (2003) Monitoring and characterisation of bacteria in corroding district heating systems using fluorescence in situ hybridisation and microautoradiography. Water Sci Technol 47:117–122.Kodama Y, Watanabe K (2004) *Sulfuricurvum kujiense* gen. nov., sp. nov., a facultatively anaerobic, chemolithoautotrophic, sulfur-oxidizing bacterium isolated from an underground crude-oil storage cavity. Int J Syst Evol Microbiol 54:2297–300.

Lee W, Lewandowski Z, Nielsen P, Hamilton W (1995) Role of sulfate-reducing bacteria in corrosion of mild steel: A review. Biofouling 8:165–194.

Lerm S, Alawi M, Miethling-Graff R, Seibt A, Wolfgramm M, Rauppach K, Würdemann H (2011a) Mikrobiologisches Monitoring in zwei geothermisch genutzten Aquiferen des Norddeutschen Beckens Microbiological monitoring of two geothermally used aquifers in the North German Basin. Zeitschr Geol Wiss 39:195–212.

Lerm S, Alawi M, Miethling-Graff R, Wolfgramm M, Rauppach K, Seibt A, Würdemann H (2011b) Influence of microbial processes on the operation of a cold store in a shallow aquifer: impact on well injectivity and filter lifetime. Grundwasser 16:93–104.

Lerm S, Westphal A, Miethling-Graff R, Alawi M, Seibt A, Wolfgramm M, Würdemann H (2013) Thermal effects on microbial composition and microbiologically induced corrosion and mineral precipitation affecting operation of a geothermal plant in a deep saline aquifer. Extremophiles 17:311–327.

Mavromatis K, Ivanova N, Anderson I, Lykidis A, Hooper SD, Sun H, Kunin V, Lapidus A, Hugenholtz P, Patel B, Kyrpides NC (2009) Genome analysis of the anaerobic thermohalophilic bacterium *Halothermothrix orenii*. PLoS ONE 4:e4192.

Miranda-Herrera C, Sauceda I, González-Sánchez J, Acuña N (2010) Corrosion degradation of pipeline carbon steels subjected to geothermal plant conditions. Anti Corrosion Methods Mater 57:167–172.

Molari M, Giovannelli D, d'Errico G, Manini E (2012) Factors influencing prokaryotic community structure composition in sub-surface coastal sediments. Estuar Coast Shelf Sci 97:141–148.

Muyzer G, de Waal EC, Uitterlinden AG (1993) Profiling of complex microbial populations by denaturing gradient gel electrophoresis analysis of polymerase chain reaction-amplified genes coding for 16S rRNA. Appl Environ Microbiol 59:695–700.

Nadkarni MA, Martin FE, Jacques NA, Hunter N (2002) Determination of bacterial load by real-time PCR using a broad-range (universal) probe and primers set. Microbiology 148:257–66.

Nelson DM, Ohene-Adjei S, Hu FS, Cann IKO, Mackie RI (2007) Bacterial diversity and distribution in the holocene sediments of a northern temperate lake. Microb Ecol 54:252–63.

Obst K, Wolfgramm M (2010) Geothermische, balneologische und speichergeologische Potenziale und Nutzungen des tieferen Untergrundes der Region Neubrandenburg. Neubrandenburg Geol Beitr 10:145–174.

Paul E, Ochoa JC, Pechaud Y, Liu Y, Liné A (2012) Effect of shear stress and growth conditions on detachment and physical properties of biofilms. Water Res 46:5499–5508. Pedersen K (1997) Microbial life in deep granitic rocks. FEMS Microbiol Rev 20:399–414.

Porter ML, Engel AS (2008) Diversity of uncultured *Epsilonproteobacteria* from terrestrial sulfidic caves and springs. Appl Environ Microbiol 74:4973–7.

Ruby EG, Jannasch HW (1982) Physiological characteristics of *Thiomicrospira* sp. strain L-12 isolated from deep-sea hydrothermal vents. J Bacteriol 149:161–165.

Sand W (2003) Microbial life in geothermal waters. Geothermics 32:655–667.

Schwieger F, Tebbe CC (1998) A new approach to utilize PCR-single-strand-conformation polymorphism for 16S rRNA gene-based microbial community analysis. Appl Environ Microbiol 64:4870–4876.

Sette LD, Simioni KCM, Vasconcellos SP, Dussan LJ, Neto EVS, Oliveira VM (2007) Analysis of the composition of bacterial communities in oil reservoirs from a southern offshore Brazilian basin. Antonie van Leeuwenhoek 91:253–66.

Sievert SM, Heidorn T, Kuever J (2000) *Halothiobacillus kellyi* sp. nov., a mesophilic, obligately chemolithoautotrophic, sulfur-oxidizing bacterium isolated from a shallow-water hydrothermal vent in the Aegean Sea, and emended description of the genus *Halothiobacillus*. Int J Syst Evol Microbiol 50:1229–37.

Sorokin DY, Tourova TP, Kolganova T V, Spiridonova EM, Berg IA, Muyzer G (2006) *Thiomicrospira halophila* sp. nov., a moderately halophilic, obligately chemolithoautotrophic, sulfur-oxidizing bacterium from hypersaline lakes. Int J Syst Evol Microbiol 56:2375–80.

Stevens T, McKinley J (1995) Lithoautotrophic microbial ecosystems in deep basalt aquifers. Science 270:450–454.

Takai K, Hirayama H, Nakagawa T, Suzuki Y, Nealson KH, Horikoshi K (2004) *Thiomicrospira thermophila* sp. nov., a novel microaerobic, thermotolerant, sulfur-oxidizing chemolithomixotroph isolated from a deep-sea hydrothermal fumarole in the TOTO caldera, Mariana Arc, Western Pacific. Int J Syst Evol Microbiol 54:2325–33.

Thompson JD, Higgins DG, Gibson TJ (1994) CLUSTAL W: improving the sensitivity of progressive multiple sequence alignment through sequence weighting, position-specific gap penalties and weight matrix choice. Nucleic Acids Res 22:4673–80.

Tourova TP, Slobodova N V, Bumazhkin BK, Kolganova T V, Muyzer G, Sorokin DY (2013) Analysis of community composition of sulfur-oxidizing bacteria in hypersaline and soda lakes using soxB as a functional molecular marker. FEMS Microbiol Ecol 84:280–9.

Valdez B, Schorr M, Quintero M, Carrillo M, Zlatev R, Stoytcheva M, Ocampo JDD (2009) Corrosion and scaling at Cerro Prieto geothermal field. Anti Corrosion Methods Mater 56:28–34.

Van Beek C (1989) Rehabilitation of clogged discharge wells in the Netherlands. Q J Eng Geol 22:75–80.

Vetter A, Mangelsdorf K, Schettler G, Seibt A, Wolfgramm M, Rauppach K, Vieth-Hillebrand A (2012) Fluid chemistry and impact of different operating modes on microbial community at Neubrandenburg heat storage (Northeast German Basin). Org Geochem 53:8–15.

Wagner M, Roger AJ, Flax JL, Gregory A, Stahl DA, Brusseau GA (1998) Phylogeny of dissimilatory sulfite reductases supports an early origin of sulfate respiration. J Bacteriol 180:2975–2983.

Wang Q, Garrity GM, Tiedje JM, Cole JR (2007) Naive Bayesian classifier for rapid assignment of rRNA sequences into the new bacterial taxonomy. Appl Environ Microbiol 73:5261–7.

Wilms R, Sass H, Köpke B, Cypionka H, Engelen B (2007) Methane and sulfate profiles within the subsurface of a tidal flat are reflected by the distribution of sulfate-reducing bacteria and methanogenic archaea. FEMS Microbiol Ecol 59:611–621.

Würdemann H, Westphal A, Lerm S, Kleyböcker A, Teitz S, Kasina M, Miethling-Graff R, Seibt A, Wolfgramm M (2014) Influence of microbial processes on the operational reliability in a geothermal heat store – Results of long-term monitoring at a full scale plant and first studies in a bypass system. Energy Procedia 59:412–417.

Ye J, Coulouris G, Zaretskaya I, Cutcutache I, Rozen S, Madden TL (2012) Primer-BLAST: a tool to design target-specific primers for polymerase chain reaction. BMC Bioi 13:134.